

A Membrane-delimited Effect of Internal pH on the K⁺ Outward Rectifier of *Vicia Faba* Guard Cells

H. Miedema, S.M. Assmann

Biology Department, The Pennsylvania State University, 208 Mueller Laboratory, University Park, PA 16802

Received: 5 June 1996/Revised: 1 August 1996

Abstract. ABA stimulation of outward K⁺ current ($I_{K,out}$) in *Vicia faba* guard cells has been correlated with a rise in cytosolic pH (pH_i). However, the underlying mechanism by which $I_{K,out}$ is affected by pH_i has remained unknown. Here, we demonstrate that pH_i regulates outward K⁺ current in isolated membrane patches from *Vicia faba* guard cells. The stimulatory effect of alkalinizing pH_i was voltage insensitive and independent of the two free calcium levels tested, 50 nM and 1 μ M. The single-channel conductance was only slightly affected by pH_i . Based on single-channel measurements, the kinetics of time-activated whole-cell current, and the analysis of current noise in whole cell recordings, we conclude that alkaline pH_i enhances the magnitude of $I_{K,out}$ by increasing the number of channels available for activation. The fact that the pH_i effect is seen in excised patches indicates that signal transduction pathways involved in the regulation of $I_{K,out}$ by pH_i , and by implication, components of hormonal signal transduction pathways that are downstream of pH_i , are membrane-delimited.

Key words: *Vicia faba* — Guard Cells — Internal pH — K⁺ outward rectifier

Introduction

Solute flow during swelling and shrinking of guard cells is mediated by ion channels, selective for either cations or anions. In recent years the signal transduction pathways involved in stomatal movement of *Vicia faba* guard cells have been studied intensively (see review Assmann, 1993). Potassium loss and stomatal closure occur in response to the stress hormone, abscisic acid (ABA). Blatt

and Armstrong (1993) used the intracellular voltage clamp technique to demonstrate that ABA enhances the magnitude of the outward K⁺ current ($I_{K,out}$) in intact guard cells. Blatt (1992) hypothesized that cytosolic pH (pH_i) plays an important role in this response, based on his observation that $I_{K,out}$ is inhibited by lowering pH_i in acid loading experiments employing intact guard cells inserted with double-barreled microelectrodes. Blatt and Armstrong (1993) elegantly demonstrated that pH_i is indeed involved in the response of the cell to ABA, as ABA-induced stimulation of $I_{K,out}$ could be suppressed by acidifying the cytoplasm. Lemitri-Chlieh and MacRobbie (1994) used the whole-cell configuration (WC) of the patch-clamp technique to study the modulation of K⁺ channels by Ca_i^{2+} and pH_i . Their finding, a stimulation of $I_{K,out}$ at more alkaline pH_i , and no effect of alterations in Ca_i^{2+} , confirmed the conclusions of Blatt (1992) and Blatt and Armstrong (1993).

While an effect of pH_i on $I_{K,out}$ thus seems obvious, several questions remain to be answered. For instance, where exactly in the cascade of signal transduction events does pH_i exert its effect on $I_{K,out}$? Can the pH_i effect be traced to occur in the cytoplasm or is its target located in the membrane? If the sensor for pH_i is indeed membrane delimited, one should expect to see an effect of pH_i in excised membrane patches as well as in intact cells. Another question concerns the mechanism of modulation of $I_{K,out}$ by pH_i . Is it the single channel conductance or open probability that is changed by pH_i or is it a change in channel availability? The aim of the present study was to address the above questions by analyzing the effect of cytosolic pH on the potassium outward rectifier at the single channel level, employing both isolated patches and analysis of current fluctuations in whole-cell recordings.

To date, relatively little single-channel analysis has been performed on the outward rectifier. Besides the preliminary study of Hosoi, Iino and Shimazaki (1988),

only Ilan, Schwartz and Moran (1994) studied $I_{K,out}$ in detail at the single-channel level. They reported an effect of external pH on $I_{K,out}$, but did not address effects of internal pH.

Materials and Methods

PLANT MATERIAL AND PROTOPLAST ISOLATION

Plants of *Vicia faba* were grown in growth chambers under a 10-hr light/14-hr dark regime at a light intensity of $0.2 \text{ mmol m}^{-2}\text{s}^{-1}$. The temperature was 20 and 18°C in light and dark, respectively. Protoplasts were isolated from 3–4 week old plants according to Kruse, Tallman and Zeiger (1989) with modifications. The following solutions were used: Blending medium (in mM): 10 MES, 5 CaCl_2 , 0.5 ascorbic acid, 0.1% polyvinylpyrrolidone (Sigma, PVP40) adjusted to pH 6 using KOH. Basic medium: 5 MES, 10 μM KH_2PO_4 , 0.5 CaCl_2 , 0.5 MgCl_2 , 0.5 ascorbic acid, 450 sorbitol, adjusted to pH 5.5 with KOH. Enzyme solution #1: 0.7% Cellulysin, *Trichoderma viride* (Calbiochem, La Jolla, CA), 0.1% PVP40, 0.25% bovine serum albumin (Sigma, St. Louis, MO), 0.5 mM ascorbic acid, dissolved in 55% (v/v) Basic medium and 45% (v/v) distilled water, pH 5.5 (KOH). Enzyme solution #2: 1.5% Cellulase, Onozuka RS (Yakult Honsha, Tokyo, Japan), 0.02% Pectolyase Y-23 (Seishin, Tokyo, Japan), 0.25% BSA, 0.5 mM ascorbic acid, in Basic medium. Prior to use, the pH of enzyme solution #2 is reduced to pH 3.5 for 5 min, using HCl, in order to inactivate protease contaminants. The pH is then raised to 5.5 using KOH. Finally, the enzyme mixture is vacuum filtered through a 0.45 μm filter (MSI, Westboro, MA).

Following removal of the major veins, 6 young, fully expanded leaves are cut into 1-cm² pieces using a razor blade. The leaf pieces are blended for 45 sec in 125 ml of Blending medium, using a commercial Waring blender connected to a Variac set to 65% of full scale. The blending step serves to remove mesophyll cells and rupture most epidermal cells. The blended mixture is poured through fine cotton mesh to remove broken mesophyll and epidermal cells. The remaining epidermal peels are rinsed thoroughly with deionized water. The peels are then transferred to a petri dish filled with deionized water to facilitate the removal of visible pieces of mesophyll tissue and other contaminants using forceps. The peels are collected again on cotton mesh and placed in a 50 ml Erlenmeyer flask containing 10 ml of enzyme solution #1. The flask is placed in a shaking water bath (American Scientific Products, #YB-521) in the dark at 27°C for 30 min, with the shaking speed set to #9. After 30 min, 30 ml Basic medium is added, then the mixture is shaken for an additional 5 min under the same conditions. The peels are collected on 220 μm nylon mesh and rinsed gently with Basic medium, then transferred into 10 ml of enzyme solution #2 in a 50 ml Erlenmeyer flask. The flask is returned to the shaking water bath, and incubated in the dark, at 17°C for 20 min, while shaking at speed #6. After 20 min, the shaking speed is reduced to #4, then incubation is continued for an additional 25 min, at which time a sample is checked for completeness of digestion. Incubation is continued until most guard cells are completely round and some have begun to move away from the stomatal pore. Typically, an incubation period of 55 min in enzyme solution #2 produces sufficient protoplasts for patch clamp purposes. After incubation, the flask is carefully shaken by hand for a few seconds, then the mixture is filtered through 220 μm nylon mesh and the cells are collected in a 50-ml centrifuge tube. Basic medium is added to give a final volume of 50 ml. Shaking by hand prior to filtering significantly improves the yield of protoplasts. The cells are subsequently spun in a benchtop centrifuge for 4

min at $200 \times g$. All but 1 ml of supernatant is carefully removed, then the protoplast pellet is resuspended in the remaining fluid. The tube is refilled with Basic medium and a second, identical centrifugation is performed. The protoplasts are kept on ice in the dark until use in patch clamp experiments.

PATCH CLAMP MEASUREMENTS

Measurements were performed using an Axopatch-1B patch clamp amplifier and a DigiData 1200 Interface (both from Axon Instruments, Foster City, CA). Unless stated otherwise, the sampling rate was 5 kHz, in both whole-cell and single channel measurements. Currents were filtered at a -3 dB frequency of 1 kHz by the four-pole Bessel filter on the Axopatch-1B. Data analysis was accomplished using PCLAMP software (version 6.0.2, Axon Instruments). Potentials are presented in terms of membrane potential, i.e., the potential at the cytosolic face of the membrane with respect to the potential at the external face. Where appropriate, potentials have been corrected for liquid junction potentials as determined in separate measurements (Barry & Lynch, 1991).

WHOLE-CELL MEASUREMENTS

The composition of the solutions was as follows (in mM). In the bath: 100 K^+ -Glutamate, 1 MgCl_2 , 1 CaCl_2 , 10 Hepes pH 7.2 and sorbitol to a final osmolality of 460 mmol kg^{-1} solution. In the pipette: 80 K^+ -Glutamate, 20 KCl, 2 MgCl_2 , 10 Hepes pH 7.2 or 7.8, 2 EGTA and sorbitol to a final osmolality of 500 mmol kg^{-1} solution. Before use, pipette and bath solutions were filtered using 0.22 μm filters (MSI, Westboro, MA). The pipette solution was supplemented with, freshly prepared, 2 Mg-ATP (Sigma). These solutions resulted in reversal potentials (corrected both for KOH added for pH adjustment and for ion activities) of -1 and +39 mV for K^+ and Cl^- , respectively. Whole-cell currents were corrected for a time-independent or leak conductance and normalized, i.e., expressed in pA/pF to eliminate differences due to variations in cell surface area (Gill et al., 1992). Variations in current levels are expressed as standard errors of the mean.

A two-stage pipette puller (Narishige, Tokyo, Japan) was used to pull pipettes using nonfilamented glass capillaries (Kimax-51, Kimble Products). For the given pipette and bath solutions, the pipette resistance was typically around 10 M Ω .

EXCISED PATCH MEASUREMENTS

The pipette solution contained (in mM): 5 KCl, 5 K^+ -Gluconate, 0.5 CaCl_2 , 10 Hepes pH 7.0. During recordings on excised inside-out patches the bath solution contained (in mM) 20 KCl, 80 K^+ -Gluconate, 2 EGTA and 10 Hepes, except for the measurements at pH_i 6.0, in which the solution contained 10 MES instead of 10 Hepes. For all solutions, the pH was adjusted with KOH and mannitol was added to a final osmolality of 450 mmol kg^{-1} . These solutions resulted in reversal potentials (corrected both for KOH addition for pH adjustment and for ion activities) of -49 and -51 mV for K^+ , at pH 7.0 and 8.0, respectively and +26 mV for Cl^- .

For the excised patch measurements, pipettes were pulled from Filamented Patch Clamp Glass (Catalog #5968, A-M Systems, Everett, WA). At the start of the experiment, the patch-clamp dish was filled with pipette solution and the pipette resistance was typically between 100–150 M Ω . After establishing an on-cell G Ω seal, an inside-out patch was pulled and the solution in the dish was then replaced by bath solution.

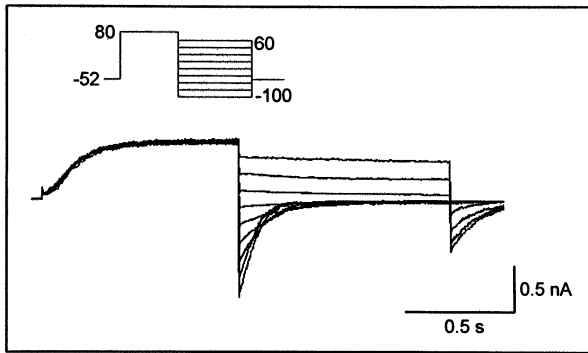


Fig. 1. Recordings from a tail-current analysis, performed to determine the reversal potential of the whole-cell outward current. Instead of 100 mM K^+ Glutamate, the bath contained 100 mM KCl. After leak subtraction, the reversal potential was derived by interpolation of the current levels. The value of E_{rev} obtained (+8 mV) indicates the K^+ selectivity of the outward current over Cl^- ($E_{K^+} = -1$ mV and $E_{Cl^-} = -37$ mV). The voltage pulse protocol is shown in the inset. The sampling rate was 1 kHz.

Results

EFFECT OF pH_i IN THE WHOLE-CELL CONFIGURATION

The identification of the ionic species that actually carries the whole-cell outward current requires the determination of the reversal potential. Figure 1 shows a tail current experiment at pH_i 7.8. The value of E_{rev} , +8 mV, indicates that the permeant ion is indeed K^+ ($E_{K^+} = -1$ mV) and not Cl^- ($E_{Cl^-} = -37$ mV). At pH_i 7.2, the reversal potential was +11 mV (*not shown*), indicating a similar selectivity of the whole-cell membrane at both pH_i s. As can be seen, E_{rev} is more positive than E_{K^+} . A similar phenomenon has been observed in guard cells of *Zea mays* and may reflect a permeability of the whole-cell membrane to Mg^{2+} (Fairley-Grenot & Assmann, 1992).

Figure 2 shows whole-cell recordings at internal pHs of 7.2 (A) and 7.8 (B) with a free Ca_i^{2+} concentration of 1 μ M. A pH_i of 7.8 resulted in a marked stimulation of outward current. The current-voltage relationships (*IV*-curves) of the data presented in Fig. 2 are shown in Fig. 3. Note that at both pH_i s the 'activation potential,' i.e., the potential at which current is first detected (*see e.g.*, Hedrich et al., 1994), of the outward (= positive) current is the same, around -20 to 0 mV. Figure 4A summarizes steady-state current levels of the time-activated currents as observed in eight (pH_i 7.2) and six (pH_i 7.8) different cells, at various holding potentials, measured 15 min after obtaining the whole-cell configuration. The variation in outward current magnitude is large, a phenomenon also observed by Lemtiri-Chlieh and MacRobbie (1994). However, despite this variation in $I_{K,out}$, the effect of pH_i is still profound. As can be seen in Fig. 4B,

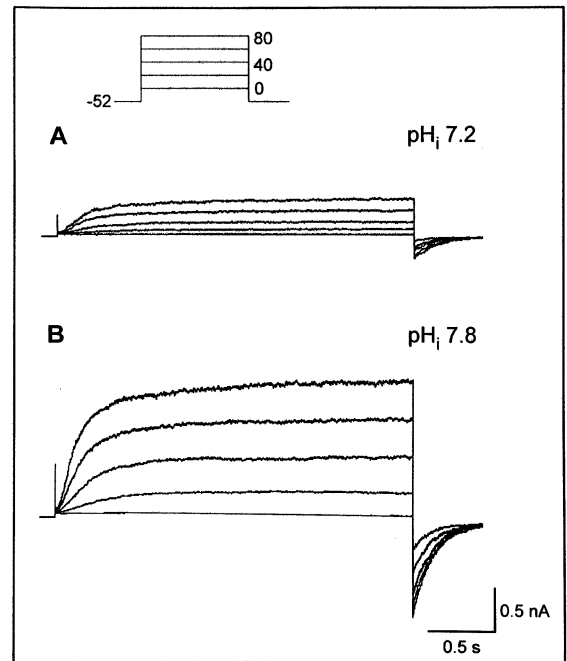


Fig. 2. Examples of whole-cell current recordings at pH_i 7.2 (A) and pH_i 7.8 (B) at different applied membrane potentials, obtained from two different cells. The voltage-pulse protocol is shown in the inset.

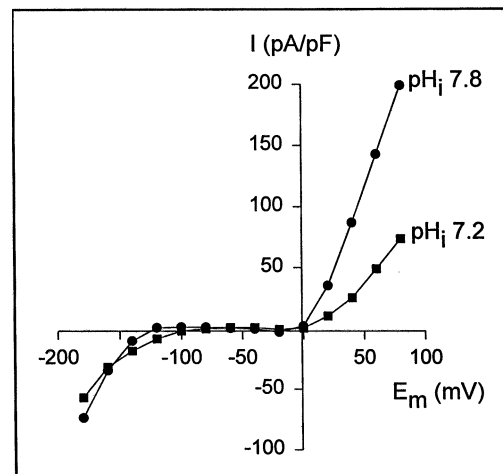


Fig. 3. Current-voltage relationships (*IV*-curves) based on the data shown in Fig. 2. Values are based on steady-state current levels 15 min after obtaining the whole-cell configuration.

the increase in $I_{K,out}$ at pH_i 7.8, based on the data shown in (A), is fairly constant and falls in a range between a 3.6-fold increase at +20 mV and a 2.9-fold increase at +80 mV. Therefore, we conclude that the effect of pH_i on the steady-state whole-cell current is, at least in the voltage range tested, just weakly voltage sensitive. From intracellular recording experiments Blatt and Armstrong (1993) reported that the effect of pH_i on $I_{K,out}$ is voltage independent.

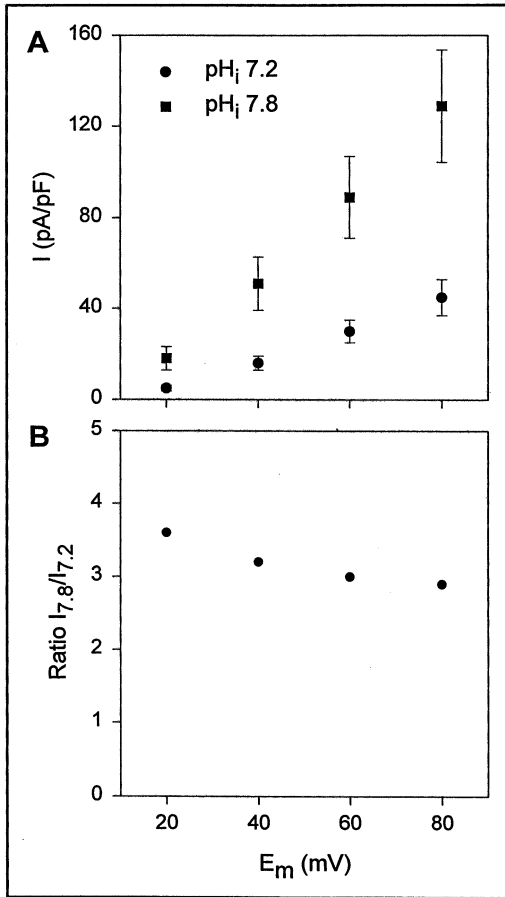


Fig. 4. (A) Average whole-cell steady-state currents at different membrane potentials, at pH_i 7.2 or 7.8 and at a free Ca_i²⁺ concentration of 1 μM. Values are based on current levels 15 min after obtaining the whole-cell configuration. Error bars represent standard errors. (B) The ratio of the average steady-state current level at pH_i 7.8 and pH_i 7.2. Values for (A) and (B) are based on the same eight (pH_i 7.2) and six experiments (pH_i 7.8).

In contrast to the effect of pH_i on the steady-state current levels of $I_{K,out}$, the inward rectifying current ($I_{K,in}$), observed at negative membrane potentials, was almost unaffected by pH_i (see Fig. 3). In the same cells as used for the analysis of $I_{K,out}$, $I_{K,in}$ was (\pm SE) -95 ± 13.8 and -111 ± 7.5 pA/pF at a pH_i of 7.2 and 7.8, respectively, measured at a membrane potential of -180 mV.

To study the effect of pH_i on $I_{K,out}$ in more detail, we performed a kinetic analysis of the time-activated outward current. The current traces could be fitted best by a sum of two exponentials (see also Ilan et al., 1994). Fits using second (Van Duijn, 1993, fitting outward currents in tobacco protoplasts from cell suspension cultures; Schroeder, 1989) or fourth order power (or sigmoidal) functions (Vogelzang & Prins, 1995, fitting outward currents in *Plantago* root protoplasts) were obviously worse (*data not shown*). Examples of double exponential fits are shown in Fig. 5, and the time

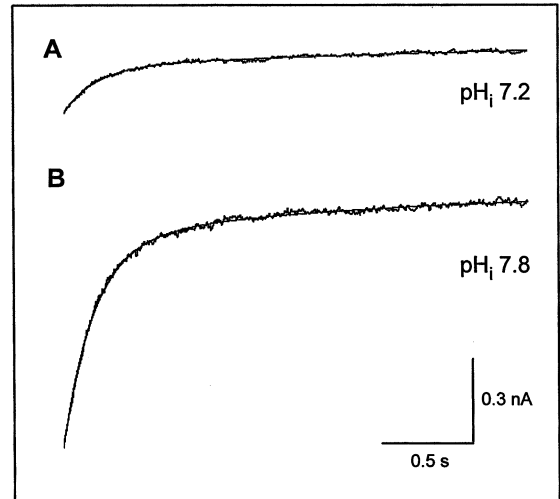


Fig. 5. Examples of time-activated whole-cell currents at a membrane potential of $+60$ mV, at an internal pH of 7.2 (A) or 7.8 (B). Current traces were fitted to the sum of two exponentials. For clarity of presentation, the current traces shown here were filtered at 100 Hz subsequent to acquisition at 1 kHz.

constants obtained from several different cells are given in Table 1. These values are in good agreement with values of 211 and 1295 msec reported by Ilan et al. (1994), measured at a membrane potential of $+63$ mV, and also with values reported by Schroeder (1989) (387 msec at $+23$ mV and 195 msec at $+81$ mV), although he used a second order power function to describe $I_{K,out}$. Considering the duration of the voltage pulse (2.5 sec), the fit will be insensitive to time constants of comparable magnitude. This expectation is confirmed when we compare the values of the two time constants with the value obtained when the traces are fit by a single instead of a double exponential. This procedure resulted in slightly lesser fits, however, the time constant obtained was around 400 msec both at pH_i 7.2 and 7.8 (*data not shown*). Apparently, the response is dominated by the small time constant. Therefore, because the average value of the small time constant is almost identical at both pH_is (207 msec at pH_i 7.2 vs. 203 msec at pH_i 7.8), it seems justified to conclude that the kinetics of channel gating are not significantly affected by pH_i, despite the scatter in the larger time constant.

SINGLE-CHANNEL MEASUREMENTS

Selectivity and Voltage Sensitivity of $I_{K,out}$

Figure 6 shows current recordings in the inside-out patch (IOP) configuration at different applied membrane potentials, at pH_i 8.0 and at a free Ca_i²⁺ concentration of 1 μM. The IV-curve based on the data in Fig. 6 is shown in

Table 1. Time constants (in msec) resulting from fitting the time-activated outward currents at a membrane potential of +60 mV to the sum of two exponentials for six (pH_i 7.2) and five (pH_i 7.8) different cells

Exp. No	pH 7.2		pH 7.8	
	τ_1	τ_2	τ_1	τ_2
1	332	639	129	1152
2	140	450	163	1559
3	194	7016	277	897
4	200	2887	263	2069
5	85	735	183	811
6	290	8864		
Mean	207	3432	203	1298
SE	37.6	1490	28.6	232.6

The time interval used for the fit of each current trace was between 160 and 2500 msec after the start of the 2.5-sec voltage pulse. For the fitting procedure we used the Chebyshev algorithm in PCLAMP 6.0.2. When using the SIMPLEX algorithm, the fit was either obviously worse, when all parameters were allowed to vary, or rather sensitive (and therefore arbitrary), depending on the chosen, fixed values of one or more parameters.

Fig. 7. Linear regression of the data points resulted in a single channel conductance of 27 pS. The observed reversal potential of -45 mV is close to E_{K^+} (-51 mV under these conditions) indicating the K^+ selectivity of the channel. Qualitatively, the voltage activation of $I_{K,out}$ at the single channel level (Fig. 6) is similar to the observed voltage dependence in WC (Fig. 3). In excised patches, the channel consistently inactivated completely at membrane potentials more negative than -20 to -30 mV.

Effect of pH_i on $I_{K,out}$ in Excised Patches

A valid comparison of whole-cell and single-channel measurements first requires confirmation that the channel studied at the isolated patch level is indeed responsible for the whole cell current. The similarity in voltage sensitivity of the current observed in WC and IOP, described above, is the first piece of evidence that the channel studied in both configurations is indeed one and the same. A second piece of evidence is the K^+ over Cl^- selectivity observed in both configurations (Fig. 1, Table 2). Table 2 summarizes effects of pH_i on single-channel characteristics in the IOP configuration and under different Ca_i^{2+} concentrations. Under the isolated patch conditions, E_{K^+} is -49 mV at pH_i 7.0 and -51 mV at pH_i 8.0, while E_{Cl^-} is +26 mV. From these values and from the measured reversal potentials (E_{rev}) in Table 2, the selectivity of the channel for K^+ over Cl^- is obvious. The permeability ratio P_{K^+}/P_{Cl^-} based on the range of reversal potentials is between 4.0 and 5.5. As can be seen, there is no significant effect of pH_i on E_{rev} . A second

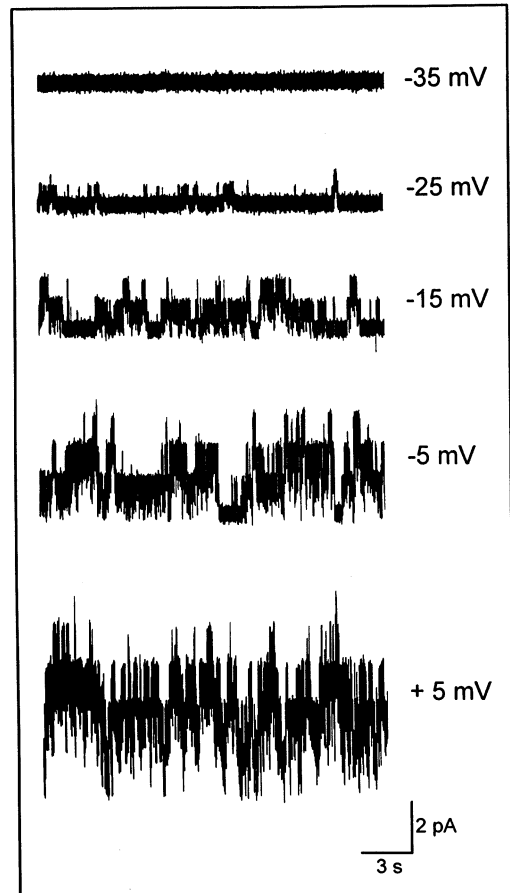


Fig. 6. Single-channel current traces of 20-sec duration in an excised inside-out patch at different applied membrane potentials, at pH_i 8 and at a free Ca_i^{2+} concentration of 1 μ M. Upward current deflections reflect channel opening.

conclusion based on the data in Table 2 is that the free Ca_i^{2+} concentration does not affect g or E_{rev} . A lack of effect of internal calcium on $I_{K,out}$ has been reported frequently (Blatt, Thiel & Trentham, 1990; Hosoi et al., 1988; Schroeder & Hagiwara, 1989). The similarity in calcium insensitivity of $I_{K,out}$ in the whole-cell and in the excised membrane provides the third piece of evidence that the same channel is being studied.

Figure 8 shows single-channel recordings at three physiological pH_i: pH_i 7.5, 7.2 and 7.8, at a membrane potential of -15 mV and at a free Ca_i^{2+} concentration of 1 μ M. As observed in the whole-cell configuration, at the single channel level $I_{K,out}$ showed a strong pH_i dependence. Switching pH_i from 7.5 to 7.2 strongly inactivated the channel, an inactivation that could be reversed by pH_i 7.8. A similar insensitivity of $I_{K,out}$ to pH_i was observed at a Ca_i^{2+} concentration of 50 nM (Fig. 9). Figure 9 shows current recordings of an inside-out patch at a membrane potential of -15 mV, sequentially exposed to pH_i 7.0, 6.0, again 7.0 and 8.0. The recordings in Figs.

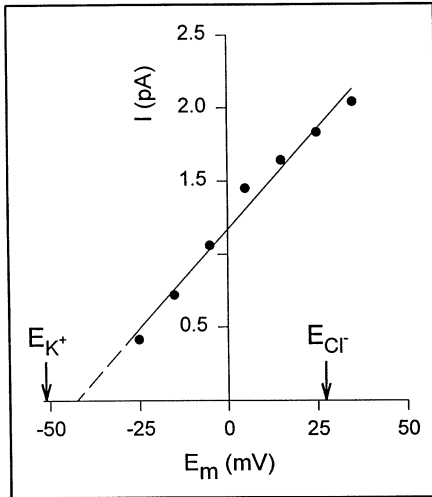


Fig. 7. IV-curve based on the data shown in Fig. 5. Linear regression of the data points resulted in a single-channel conductance of 27 pS and a reversal potential of -45 mV, indicating the selectivity of the channel for K^+ over Cl^- . Nernst potentials of K^+ and Cl^- are indicated by arrows.

Table 2. Average values of single-channel conductance (g) and reversal potential (E_{rev}), as recorded in inside-out patches at a pH_i of 7.0 and 8.0 and at either 50 nM or 1 μ M free Ca_i^{2+}

	g in pS	E_{rev} in mV	n
pH_i 7, 50 nM Ca_i^{2+}	24 (1.0)	-43 (1.5)	11
pH_i 7, 1 μ M Ca_i^{2+}	25 (1.6)	-44 (1.5)	2
pH_i 8, 50 nM Ca_i^{2+}	29 (0.9)	-44 (1.3)	7
pH_i 8, 1 μ M Ca_i^{2+}	29 (1.1)	-44 (0.9)	7

Standard errors are given in parentheses and the last column contains the number of experiments on which the data are based. Theoretical reversal potentials: E_{K^+} is -49 mV at pH_i 7.0 and -51 mV at pH_i 8.0; E_{Cl^-} is $+26$ mV. From these values and from E_{rev} the permeability ratio P_{K^+}/P_{Cl^-} based on the range of E_{rev} is between 4.0 and 5.5.

8 and 9 illustrate, first, that the inhibition by low pH_i is reversible and, second, that, qualitatively, the effect of pH_i is independent of the calcium level, at least within the conditions tested. While the free Ca_i^{2+} concentration has no effect on g , a minor effect of pH_i on g was observed: compared to pH_i 7.0, at pH_i 8.0 g increased approximately 1.2-fold (Table 2). This minor effect is not sufficient to account for the large, threefold increase in $I_{K,out}$ observed in WC recordings (Fig. 2–4). Our range of conductance values, 24 to 29 pS, is within the range reported by Hosoi et al., (1988) of 10–30 pS, as measured in symmetrical 50 mM KCl and with an internal and external pH of 7.2. In contrast, under comparable experimental conditions as we employed for our measurements, Ilan et al. (1994) found single channel conductances of 9.1 and 10.5 pS at pH_o 5.5 and 4.4, respec-

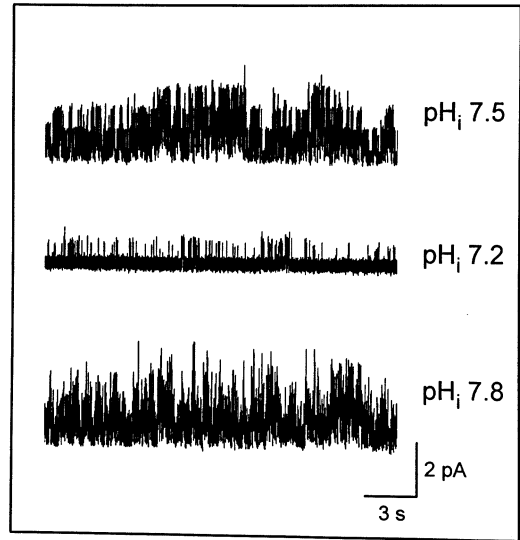


Fig. 8. Single-channel recordings of an inside-out patch at a membrane potential of -15 mV, sequentially exposed to a bath pH of 7.5, 7.2 and 7.8, and at a free Ca_i^{2+} concentration of 1 μ M. Upward current deflections reflect channel opening.

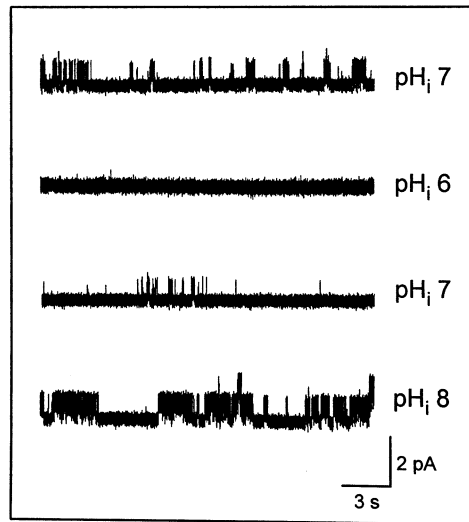


Fig. 9. Single-channel recordings of an inside-out patch at a membrane potential of -15 mV, sequentially exposed to a bath pH of 7.0, 6.0, again 7.0 and 8.0, and at a free Ca_i^{2+} concentration of 50 nM. Upward current deflections reflect channel opening.

tively, values less than half the values we find at an external pH of 7.0.

In contrast to the minor effect of pH_i on the single-channel conductance, channel activity, expressed as total open probability, was significantly increased at more alkaline pH_i . Table 3 summarizes the effect of pH_i on the total open probability of $I_{K,out}$ as obtained in five independent measurements. The total open probability is de-

Table 3. Calculated total open probabilities at pH_i 7.0 and 8.0 and their ratio as observed in five different inside-out patches

Exp. No	pH _i 7.0	pH _i 8.0	Ratio
1	0.42	1.68	4.0
2	0.16	0.32	2.0
3	0.50	1.25	2.5
4	0.15	0.36	2.5
5	0.18	0.27	1.5

The open probability is expressed as $\sum nP_o$, where P_o refers to the probability of n open channels. Values are based on recordings of either 20- or 200-sec duration. Membrane potential and free Ca_i²⁺ concentration were -15 mV and 50 nM, respectively.

defined as $\sum nP_o$ where P_o refers to the probability of n simultaneously open channels. The observed variation in this value within a given pH_i may (partly) result from variation in the total number of channels present in a patch. Given this variation, the effect of pH_i on $I_{K,out}$ is expressed as the ratio of $\sum nP_o$ at pH_i 8.0 and $\sum nP_o$ at pH_i 7.0. On average, switching from pH_i 7.0 to pH_i 8.0 resulted in a 2.5-fold increase in $\sum nP_o$.

Noise Analysis of Whole-Cell Currents

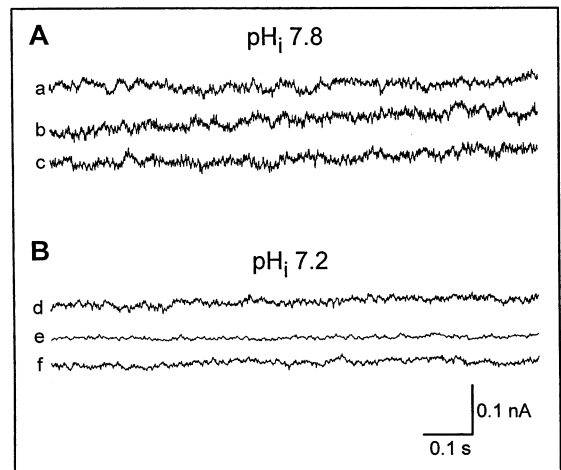
Single-channel measurements led us to conclude that pH_i modulation of $I_{K,out}$ occurs by affecting $\sum nP_o$ rather than by altering the single-channel conductance g . As we will see in this section, the same conclusion can be derived from an analysis of the whole-cell current noise. Standard noise analysis requires independent channel gating (*see* Appendix). Most frequently, we found either no channels (or at least no activity) or at least four or five channels in the membrane patch (*see* e.g. Fig. 6, lowest trace; Fig. 9, the observation of only two open channels at pH_i 8.0 in the lowest trace was in this respect unusual). The occurrence of multiple channels in excised patches may suggest that the channel is not distributed randomly but that it is located in clusters in the membrane. As pointed out by Draber, Schultze & Hansen (1993), then, it is conceivable that the channels do not gate independently but act in a cooperative way, due to some mechanical or electrostatic interaction. However, there was no statistical difference (χ^2 -test) between the observed probability of n open channels and values predicted by the binomial distribution (*data not shown*), leading to the conclusion that channel gating is indeed independent.

During a whole-cell recording different sources contribute to the observed, total current noise. As explained in the Appendix each of these noise sources can be quantified, finally resulting in an estimation of the noise associated with channel gating (σ_{gating}^2). Table 4 contains calculated values of σ_{gating}^2 derived from steady-state current segments of 1-sec duration (e.g., as in Fig. 10, at different membrane potentials and at pH_i 7.2 and 7.8.

Table 4. Calculated gating noise (σ_{gating}^2) in whole-cell current recordings at different membrane potentials (E_m), at a pH_i of 7.2 and 7.8 and at a free Ca_i²⁺ concentration of 1 μ M

E_m	pH _i 7.2	pH _i 7.8	Ratio
+20 mV	55	123	2.2
+40 mV	204	640	3.1
+60 mV	335	1300	3.9
+80 mV	694	1932	2.8

The ratio given in the last column is defined as the value of σ_{gating}^2 at pH_i 7.8 divided by its value at pH_i 7.2. Values are expressed in A² ($\times 10^{25}$) and are based on eleven (pH_i 7.2) and six different cells (pH_i 7.8). The data are based on comparable steady-state current levels, rather than on current levels measured 15 min after obtaining the whole cell configuration, as was done for the data in Fig. 4.

**Fig. 10.** Examples of whole cell current segments of 1-sec duration used for noise analysis. Recordings are from three separate cells at pH_i 7.8 (a-c) and three cells at pH_i 7.2 (d-f). E_m is +60 mV in all cases.

According to Eq. 6 (*see* Appendix), σ_{gating}^2 will increase with the square of the single-channel current (i). Therefore, if the observed threefold increase of the whole-cell current at pH 7.8 (Fig. 4) would be solely the result of an increase of i one would expect a ninefold increase in σ_{gating}^2 . However, compared to pH_i 7.2, at pH_i 7.8 σ_{gating}^2 is increased by, at most 3.9 (at +60 mV). Therefore, we conclude, consistent with the single-channel data, that a change in single-channel conductance alone cannot account for the increase of $I_{K,out}$ at pH_i 7.8. As at both pH_is the average whole-cell capacitance was approximately the same (*data not shown*), it is unlikely that variations in σ_{gating}^2 are due to differences in the total number of channels present in the whole-cell membrane.

Theoretically, both $\sum nP_o$ and σ_{gating}^2 will be changed either by a shift in the open probability of individual channels (p_o) or by a shift in the number of activated channels (n). However, the fact that the activation time

constants of $I_{K,out}$ remain the same at pH_i 7.2 and 7.8 (Fig. 5, Table 1) implies an effect of pH_i on n rather than on p_o (see Discussion).

One could argue that filtering at 1 kHz prevented detection of additional gating noise at pH_i 7.8 that resulted from a shift in σ_{gating}^2 to a frequency above the experimental filter cutoff of 1 kHz. However, as the theoretical cutoff frequency of the current signal is a function of the mean closed and open times of the channel only and is thus independent of n (see Appendix), the bandwidth of σ_{gating}^2 will change only if the activation kinetics of the current change. Since pH_i does not, in fact, change the activation kinetics (Fig. 5, Table 1), the bandwidth of σ_{gating}^2 for $I_{K,out}$ will be unaffected by pH_i .

Discussion

pH_i AND TRANSDUCTION OF HORMONAL SIGNALS IN GUARD CELLS

As ABA induces a rise in cytosolic pH (Blatt & Armstrong, 1993; Irving, Gehring & Parish, 1992), it has been postulated that pH_i is the second messenger for ABA and is responsible for the modulation of $I_{K,out}$. Elevation of pH_i has been demonstrated to stimulate the K^+ outward rectifier in intact guard cells (Blatt & Armstrong, 1993) and in guard cell protoplasts in the whole cell configuration (Lemtiri-Chlieh & MacRobbie, 1994). However, the mechanism underlying this pH_i effect has remained unknown. The present paper shows, for the first time, that effects of pH_i on $I_{K,out}$ are preserved in isolated membrane patches. These results therefore suggest that the portion of the signal transduction pathway for ABA that is downstream of pH_i is membrane-delimited, i.e., retained in the isolated patch.

A membrane-delimited locus of pH_i action during ABA response is somewhat difficult to reconcile with the data of Armstrong et al. (1995). They observed that in tobacco transformed with the dominant transgene, *abi1-1*, which renders stomata insensitive to ABA (Leung et al., 1994; Meyer, Leube & Grill, 1994), ABA still initiated cytosolic alkalization, yet no effects of this pH_i change on outward current were observed. Their results are therefore consistent with a pathway in which ABI1 functions downstream of the pH increase; when *abi1-1* is present, pH_i then has no effect. Yet *ABI1* is known to encode a PP2C-type phosphatase, thought to be localized in the cytosol, suggesting that it should be upstream, not downstream of the (membrane-delimited) pH_i effect. The two studies may be reconciled by postulating either a membrane-associated form of ABI1, or a species difference (tobacco vs. *Vicia faba*) in the ability of the outward rectifier to be modulated by pH_i . Since Armstrong et al. (1995) also did not detect an ABA-

stimulated increase in cytosolic Ca^{2+} , yet this increase is known to occur in other species at least some of the time (Gilroy et al., 1991; McAinsh, Brownlee & Hetherington, 1990), it does seem possible that tobacco guard cells have a different mechanism of ABA response.

A third way to reconcile the two datasets would be to argue that, while an effect of pH_i on the isolated membrane patch can be observed, such effects do not actually occur in the whole cell, where another modulatory mechanism of pH_i predominates. However, our conclusions based on single-channel measurements are in good agreement with those obtained from whole-cell noise analysis. Both single-channel measurements and whole-cell noise analysis indicate that a change in g cannot account for the increase in $I_{K,out}$ at high pH_i . The increase in total open probability in single-channel recordings is as predicted by the scalar increase in $I_{K,out}$ produced in whole-cell treatments with elevated pH_i .

THE MECHANISM OF PROTON ACTION

One way protons may modulate channel activity is by an electric screening of surface charges such that the voltage experienced by the channel differs from the actual applied voltage, resulting in a shift of the observed reversal potential (Hille, 1992). From the fact that E_{rev} is insensitive to pH_i (Table 2), we conclude that this mechanism is not responsible for the pH_i effect on $I_{K,out}$.

Our measurements at the single-channel level showed a 1.2-fold increase in single-channel conductance after switching from pH_i 7.0 to pH_i 8.0 (Table 2). Such a slight effect of pH_i on g cannot account for the observed threefold increase in the whole-cell steady-state current under even less extreme conditions, pH_i 7.2 and 7.8 (Fig. 4), indicating that a pH_i -mediated alteration of g was not responsible for the whole-cell effects observed. In contrast to the weak effect of pH_i on single-channel conductance, total channel open probability significantly increased at more alkaline pH_i , on average 2.5-fold after switching from pH_i 7.0 to pH_i 8.0.

Despite a profound effect on the magnitude of the steady-state whole-cell outward current, pH_i does not have an effect on the activation kinetics of $I_{K,out}$. The implication of these findings in relation to the observed pH_i -induced increase in total open probability at the single-channel level is significant. A change in the open probability of individual channels must be accompanied by a change in gating kinetics which will be reflected in a change in the time constant(s) of the whole-cell current. Because of the absence of such an effect, the change in total open probability at high pH_i must be interpreted as an effect on the mobilization of channels from an inactivated state to an activated, but still nonconducting state. As a result, the number of channels available for activation increases. Interestingly, to explain the voltage inde-

pendent stimulation of $I_{K,out}$ upon the addition of ABA, Blatt (1990) hypothesized either a recruitment of channels or an effect on the single-channel conductance. At the moment, a direct effect of ABA on the single-channel conductance cannot be excluded, however, Blatt's results considered with the results in the present paper indicate that ABA, by increasing pH_i , affects the number of channels actually available for activation.

ABSOLUTE VS. RELATIVE pH_i EFFECTS

A difficulty in the study of the outward rectifier, especially at the single-channel level, is its unpredictable gating behavior, a phenomenon also noticed by Ilan et al. (1994). The effect of pH_i was so strong that, despite this uncontrolled behavior, stimulation of channel activity by alkalization was still obvious and reproducible. However, this unpredictability prevents the analysis of $I_{K,out}$ in more detail, e.g., with respect to a quantitative description of the voltage sensitivity and with respect to open and closed time distributions. The seemingly uncontrolled gating at the single-channel level may underlie the huge variation in whole-cell outward current as observed here and in the measurements of Lemtiri-Chlieh and MacRobbie (1994). It may be that, besides voltage and pH_i , there is another, hidden and ill-controlled factor involved in the regulation of $I_{K,out}$ (see Ilan et al., 1994).

Taking the microelectrode measurements of Blatt and Armstrong (1992), the patch-clamp whole-cell measurements of Lemtiri-Chlieh and MacRobbie (1994), and the single-channel measurements on $I_{K,out}$ reported here as a whole leads to the hypothesis that it may be the shift in pH_i rather than the absolute value of pH_i that modulates the outward rectifier. In the measurements of Lemtiri-Chlieh and MacRobbie (1994), $I_{K,out}$ is totally inactivated at pH_i 7.2. In our recordings and in the measurements of Armstrong and Blatt (1992), there is still a significant outward current at pH_i 7.2. We observed an analogous behavior in the excised patch measurements. In some patches, pH_i 7.2 totally suppressed channel activity, while in others even pH_i 7.0 still allowed observation of some channel activity. One might argue that patches in which total suppression was seen were those which contained only one or a few channels. However, the number of channels seen at high pH_i was consistently four or five. Therefore, it seems unlikely that a difference in the total number of channels in the membrane patches can account for the variability in channel activity which was observed at high as well as low pH_i . Instead, a relative pH_i effect may explain the difference in channel activity at pH_i 7.0 before and after exposure to pH_i 6.0 (Fig. 9). Switching from pH_i 6.0 to pH_i 7.0 results in just a partial recovery of channel activity. Apparently, it is not the absolute pH_i alone that determines channel

gating; history plays a role as well. Chraïbi et al. (1995) similarly reported for the nonselective cation channel in the renal tubule of the mouse that the pH producing maximal channel activity was variable, yet the general pH effect was quite reproducible. The same is true of our studies on the guard cell $I_{K,out}$ channel; the relative pH_i effect was very consistent and profound. A change of 0.3 pH_i units sufficed to almost completely inactivate the channel (Fig. 8). Blatt and Armstrong (1993) reported a pH_i dependence even sharper than the one reported here. They found a stimulation of $I_{K,out}$ of 250% after an elevation of pH_i of just 0.16 units. From the steep pH_i dependence of the whole cell outward current, Blatt (1992) calculated a Hill coefficient of at least two. Such a strong dependence of $I_{K,out}$ on pH_i indicates that pH_i can be a major regulator of $I_{K,out}$ despite the limited fluctuations of pH_i *in vivo*.

The authors thank Dr. Lisa A. Romano for the data presented in Fig. 1. This research was supported by NSF grant MCB-9316319 and USDA grant 92-37100-8333 to S.M. Assmann.

References

- Armstrong, F., Leung, J., Grabov, A., Brearley, J., Giraudat, J., Blatt, M.R. 1995. Sensitivity to abscisic acid of guard cell K^+ channels is suppressed by *abi1-1*, a mutant *Arabidopsis* gene encoding a putative protein phosphatase. *Proc. Natl. Acad. Sci. USA* **92**:9520–9524
- Assmann, S.M. 1993. Signal transduction in guard cells. *Annu. Rev. Cell Biol.* **9**:345–375
- Barry, P.H., Lynch, J.W. 1991. Liquid junction potentials and small cell effects in patch clamp analysis. *J. Membrane Biol.* **121**:101–117
- Blatt, M.R. 1990. Potassium channel currents in intact stomatal guard cells: rapid enhancement by abscisic acid. *Planta* **180**:445–455
- Blatt, M.R. 1992. K^+ channels of stomatal guard cells. Characteristics of the inward rectifier and its control by pH. *J. Gen. Physiol.* **99**:615–644
- Blatt, M.R., Armstrong, F. 1993. K^+ channels of stomatal guard cells: abscisic-acid-evoked control of the outward rectifier mediated by cytoplasmic pH. *Planta* **191**:330–341
- Blatt, M.R., Thiel, G., Trentham, D.R. 1990. Reversible inactivation of K^+ channels of *Vicia* stomatal guard cells following the photolysis of caged inositol 1,4,5-triphosphate. *Nature* **346**:766–769
- Chraïbi, A., Guinamard, R., Teulon, J. 1995. Effects of internal pH on the nonselective cation channel from the mouse collecting tubule. *J. Membrane Biol.* **148**:83–90
- Dempster, J. 1993. Computer analysis of electrophysiological signals. Academic Press, San Diego, CA
- Draber, S., Schultze, R., Hansen, U-P. 1993. Cooperative behavior of K^+ channels in the tonoplast of *Chara corallina*. *Biophys. J.* **65**:1553–1559
- Fairley-Grenot, K.A., Assmann, S.M. 1992. Whole cell K^+ current across the plasma membrane of guard cells from a grass: *Zea mays*. *Planta* **186**:282–293

- Gill, D.R., Hyde, S.C., Higgins, C.F., Valverde, M.A., Mintenig, G.M., Sepulveda, F.V. 1992. Separation of drug transport and chloride channel functions of the human multidrug resistance P-glycoprotein. *Cell* **71**:23–32
- Gilroy, S., Fricker, M.D., Read, N.D., Trewavas, A.J. 1991. Role of calcium in signal transduction of *Commelina* guard cells. *Plant Cell* **3**:333–344
- Hedrich, R., Marten, I., Lohse, G., Dietrich, P., Winter, H., Lohaus, G., Heldt, H-W. 1994. Malate-sensitive anion channels enable guard cells to sense changes in the ambient CO₂ concentration. *Plant J.* **6**:741–748
- Hille, B. 1992. Ionic channels of excitable membranes. Sinauer Associates, Sunderland, MA
- Hosoi, S., Iino, M., Shimazaki, K. 1988. Outward-rectifying K⁺ channels in stomatal guard cell protoplasts. *Plant Cell Physiol.* **29**:907–911
- Ilan, N., Schwartz, A., Moran, N. 1994. External pH effects on the depolarization-activated K channels in guard cell protoplasts of *Vicia faba*. *J. Gen. Physiol.* **103**:807–831
- Irving, H.R., Gehring, C.A., Parish, R.W. 1992. Changes in cytosolic pH and calcium of guard cells precede stomatal movements. *Proc. Natl. Acad. Sci. USA* **89**:1790–1794
- Kruse, T., Tallman, G., Zeiger, E. 1989. Isolation of guard cell protoplasts from mechanically prepared epidermis of *Vicia faba* leaves. *Plant Physiol.* **90**:1382–1386
- Lentiri-Chlieh, F., MacRobbie, M.A.C. 1994. Role of calcium in the modulation of *Vicia* guard cell potassium channels by abscisic acid: a patch-clamp study. *J. Membrane Biol.* **137**:99–107
- Leung, J., Bouvier-Durand, M., Morris, P.C., Guerrier, D., Chefdor, F., Giraudat, J. 1994. *Arabidopsis* ABA response gene *ABI1*: features of a calcium-modulated protein phosphatase. *Science* **264**:1448–1452
- Marty, A., Neher, E. 1985. Tight-seal whole-cell recording. In: Single-Channel Recording. B. Sakmann and E. Neher, editors. pp. 107–122. Plenum, New York, 2nd edition
- McAinsh, M.R., Brownlee, A.M., Hetherington, A.M. 1990. Abscisic acid induced elevation of guard cell calcium precedes stomatal closure. *Nature* **343**:186–188
- Meyer, K., Leube, M.P., Grill, E. 1994. A protein phosphatase 2C involved in ABA signal transduction in *Arabidopsis thaliana*. *Science* **264**:1452–1455
- Schroeder, J.I. 1989. Quantitative analysis of outward rectifying K⁺ channel currents in guard cell protoplasts from *Vicia faba*. *J. Membrane Biol.* **107**:229–235
- Schroeder, I., Hagiwara, S. 1989. Cytosolic calcium regulates ion channels in the plasma membrane of *Vicia faba* guard cells. *Nature* **338**:427–430
- Sigworth, F.J. 1980. The variance of sodium current fluctuations at the node of Ranvier. *J. Physiol.* **307**:97–129
- Stevens, C.F. 1977. Study of membrane permeability changes by fluctuation analysis. *Nature* **270**:391–396
- Tyerman, S.D., Whitehead, L.F., Day, D.A. 1995. A channel-like transporter for NH₄⁺ on the symbiotic interface of N₂-fixing plants. *Nature* **378**:629–632
- Van Duijn, B. 1993. Hodgkin-Huxley analysis of whole-cell outward rectifying K⁺ currents in protoplasts from tobacco cell suspension cultures. *J. Membrane Biol.* **132**:77–85.
- Vogelzang, S.A., Prins, H.B.A. 1995. Kinetic analysis of two simultaneously activated K⁺ currents in root protoplasts of *Plantago media* L. *J. Membrane Biol.* **146**:59–71

Appendix

NOISE ANALYSIS OF WHOLE-CELL RECORDINGS

In an electrically silent membrane, i.e., in a situation where channels are inactivated, the combination of series resistance (R_s) and membrane capacitance (C_m) contributes most to the background noise in a whole cell current recording (Marty & Neher, 1983). The noise introduced by R_s and C_m (σ_{series}^2) at a frequency f is:

$$\sigma_{\text{series}}^2 = 4 kTR_s(2\pi fC_m)^2 / (1 + (2\pi fR_sC_m)^2) \quad (1)$$

To calculate the total noise at a bandwidth B , Eq. 1 has to be integrated:

$$\sigma_{\text{series}}^2 = \int_0^B 4 kTR_s(2\pi fC_m)^2 / (1 + (2\pi fR_sC_m)^2) df \quad (2)$$

The numerical representation of Eq. 2 is

$$\sigma_{\text{series}}^2 = \sum_{f=0}^B 4 kTR_sC_m(2\pi fC_m)^2 / (1 + (2\pi fR_sC_m)^2) \Delta f \quad (3)$$

Employing a bandwidth of 0-999 Hz, we used a PASCAL routine to calculate σ_{series}^2 according to Eq. 3.

A second source of background noise is the membrane conductance (G) responsible for the so-called Johnson or conductance noise (σ_{cond}^2). For a given bandwidth B , σ_{cond}^2 is expressed by:

$$\sigma_{\text{cond}}^2 = 4kTBG \quad (4)$$

In our experiments σ_{cond}^2 was calculated for each individual cell, using the whole-cell conductance derived from the steady-state current levels at membrane potentials of +20, +40, +60, and +80 mV.

In a membrane containing activated channels, current fluctuations due to the gating behavior of channels will be another contributor to the observed total current noise. We will assign σ_{gating}^2 to the noise associated with channel gating. To obtain σ_{gating}^2 the background noise ($\sigma_{\text{series}}^2 + \sigma_{\text{cond}}^2$) is subtracted from the observed total noise (σ_{obs}^2):

$$\sigma_{\text{gating}}^2 = \sigma_{\text{obs}}^2 - \sigma_{\text{series}}^2 - \sigma_{\text{cond}}^2 \quad (5)$$

As pointed out by Sigworth (1980), such a subtraction implies that the different sources of current noise are uncorrelated.

σ_{obs}^2 was calculated with PCLAMP 6.0.2 by using the data acquired during the last second of the voltage clamp protocol. Table 5 contains measured values of σ_{obs}^2 and calculated values of σ_{series}^2 , σ_{cond}^2 and σ_{gating}^2 . From Table 5 it is obvious that compared to σ_{gating}^2 , the contribution of the two other noise sources, σ_{series}^2 and σ_{cond}^2 , is of minor significance, at least for frequencies below 1 kHz. Marty and Neher (1985), studying a different cell type with frequencies below 1 kHz, came to a similar conclusion.

We are particularly interested in σ_{gating}^2 as this parameter is a function of single-channel current (i), and thus g , and the open probability. The relation between σ_{gating}^2 , i , p_o and the total number of channels (N) is (Hille, 1992; Stevens, 1977; Tyerman, Whitehead & Day, 1995):

Table 5. Observed total noise (σ_{obs}^2) and calculated values of conductance noise (σ_{cond}^2) and of noise due to the combination of series resistance and whole cell capacitance (σ_{series}^2) in whole cell current recordings at a membrane potential of +20 mV

	σ_{obs}^2	σ_{cond}^2	σ_{series}^2	σ_{gating}^2
pH _i 7.2	56.8	0.5	1.1	55.2
pH _i 7.8	126.0	1.8	1.1	123.1

σ_{gating}^2 was calculated by subtracting σ_{cond}^2 and σ_{series}^2 from σ_{obs}^2 . Variances are expressed in A² ($\times 10^{25}$) and are based on eleven (pH_i 7.2) and six different cells (pH_i 7.8). Free Ca_i²⁺ concentration was 1 μM .

$$\sigma_{\text{gating}}^2 = Np_o i^2 (1 - p_o) \quad (6)$$

Equation 6 is based on the assumptions that: (i) channels exist in a single conducting state or a nonconducting state; (ii) channels gate independently and; (iii) the channel population is homogeneous (Sigworth, 1980). Differentiation of σ_{gating}^2 with respect to p_o yields:

$$\frac{\partial \sigma_{\text{gating}}^2}{\partial p_o} = Ni^2(1 - p_o) - Ni^2 p_o = Ni^2 - 2Ni^2 p_o \quad (7)$$

Equations 6 and 7 imply that σ_{gating}^2 is symmetrical around its maximal level at $p_o = 0.5$, where $\partial \sigma_{\text{gating}}^2 / \partial p_o = 0$.

The voltage activated outward rectifier in *Vicia faba* does not show significant signs of inactivation, even during periods of cell depolarizations as long as 10 min (Schroeder, 1989). Therefore, to analyze the current noise, stationary noise analysis can be performed. The bandwidth of gating noise depends on the channel gating kinetics. The cutoff or half-power frequency (f_c) of the gating noise is related to the mean open time (τ_o) and mean closed time (τ_c) of the channel (Dempster, 1993):

$$f_c = \frac{1/\tau_o + 1/\tau_c}{2\pi} \quad (8)$$

Hosoi et al. (1988) calculated τ_o and τ_c to be around 15 and 1 msec, respectively, measured at +20 mV. Such values result in an f_c of 170 Hz. Therefore, it seems that the cutoff frequency of 1 kHz we used during our measurements should not result in any significant loss of information.